

Dynamic Susceptibility of Classical Anharmonic Oscillator

—A Unified Oscillator Model for Order-Disorder
and Displacive Ferroelectrics—

Yositaka ONODERA

Department of Physics, Kyoto University, Kyoto

(Received August 6, 1970)

As a unified oscillator model for order-disorder and displacive ferroelectrics, we consider a system of interacting classical oscillators moving in the anharmonic potential $V(x) = Ax^4 + Bx^2$, where A is positive and B may be either positive or negative. The interaction of the oscillators is taken to be bilinear in their displacements and it is treated in the Weiss molecular-field approximation. For this model, it is shown that the exact expression can be obtained for the dynamic susceptibility above the Curie temperature. The theory is exact except for its being classical and use of the Weiss approximation; anharmonicity of the potential is perfectly taken into account. Detailed analysis is made for this system and temperature dependence of the dynamic response (including the occurrence of "soft" mode) is described on the basis of the results of numerical calculations for both $B > 0$ and $B < 0$ cases.

§ 1. Introduction and description of the model

Ferroelectric crystals are classified into two types: order-disorder and displacive ones. The purpose of the present paper is to investigate the dynamic response of these two kinds of ferroelectrics above the Curie temperature and clarify the difference of its behaviour they exhibit, by considering a simple anharmonic oscillator model. A similar study has been made by a few workers;^{1)~3)} but their theories are only qualitative or deal with the case of weak anharmonicity. In view of the importance of anharmonicity in ferroelectrics, it seems necessary to get a more explicit theory which has no restrictions on the degree of anharmonicity. The present author has succeeded in it for the model described below, though it is classical. It is believed that this is the first theoretical study of the dynamic susceptibility in which anharmonicity of the potential is perfectly taken into account.

The model we investigate in this paper is as follows: Consider first an assembly of oscillators moving in the anharmonic potential $V(x) = Ax^4 + Bx^2$, where x stands for the displacement of an oscillator. A is taken to be definitely positive, while B may be either positive or negative. The potential has one or two minima, depending on the sign of B , as depicted in Fig. 1. Suppose then that there be an interaction between these anharmonic oscillators which is bilinear in their displacements; it may be regarded as corresponding to the dipole-dipole interaction and causes instability of the system. We treat this interaction in the

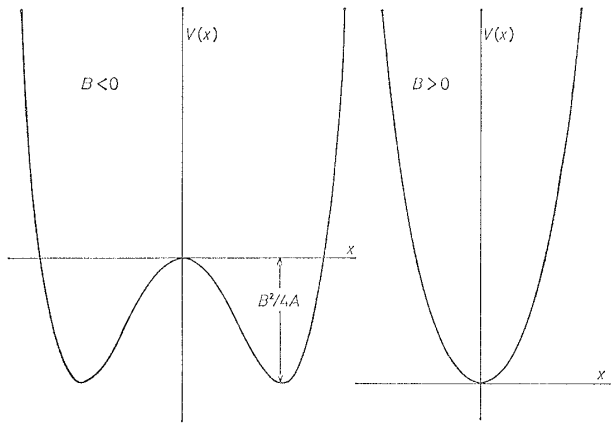


Fig. 1. Shape of the potential $V(x) = Ax^4 + Bx^2$ for $B < 0$ and $B > 0$.

framework of the Weiss molecular-field approximation. Because of the long-ranged nature of the interaction in ferroelectrics, the Weiss approximation is believed to work well. Lastly we consider the interaction of applied (alternating) electric field E with the dipole moment of the oscillator, which we assume to be proportional to its displacement.

The model system mentioned above can be described by the Hamiltonian:

$$H = H_0 + H_1,$$

$$H_0 = (M/2) \dot{x}^2 + Ax^4 + Bx^2, \quad (1.1)$$

$$H_1 = -[\gamma \langle x \rangle + E]x, \quad (1.2)$$

where M signifies the mass of the oscillator. The angular bracket means that we are to take the canonical average with respect to the total Hamiltonian H . This system undergoes a second-order phase transition in both $B < 0$ and $B > 0$ cases at a Curie temperature determined by γ . The bulk of the paper is concerned with the classical dynamic susceptibility in the paraelectric phase. In developing the theory, we shall make no approximations on the anharmonicity of the potential since we believe it essential in our problem; we pay instead the cost of the theory's being classical and of the Weiss approximation. These two restrictions are not considered critical for many ferroelectric substances, however.

A comment is here in order on the correspondence between the sign of B and the type of ferroelectric phase transition. At first sight, one may be tempted to think that the $B > 0$ case corresponds to the displacive type and $B < 0$ to the order-disorder type. It is not the case, however. When the temperature becomes much greater than $B^2/4Ak_B$ (k_B being the Boltzmann constant), the response becomes practically independent of the sign of B . The correct correspondence should therefore be

$$B > 0 \text{ or } k_B T_C \gg B^2/4A \text{ ——— displacive,}$$

$$B < 0 \text{ and } k_B T_C \lesssim B^2/4A \text{ ——— order-disorder.}$$

The final purpose of the paper is to give the spectra of dynamic response above the Curie temperature. To this end, we begin with deriving a formal expression for the dynamic susceptibility by use of the linear-response theory (§ 2). The next section (§ 3) is devoted to discussing the static properties—

temperature dependence of the static susceptibility. As shown explicitly in § 2, the solution for free oscillation is needed to evaluate the dynamic susceptibility. This is given in § 4 in terms of the Jacobian elliptic functions, together with its important characteristics. By using this result, the dynamic susceptibility is calculated in § 5. To carry through the calculation exactly, it inevitably becomes somewhat complicated, but the final expression for the dynamic susceptibility is seen to contain the contributions of various harmonics in quite a natural form. In § 6, we consider the $\omega \rightarrow 0$ limit of the dynamic susceptibility thus obtained and compare it with the static one given in § 3. It will be seen that for the $B < 0$ case the two values of the static susceptibility do not agree (owing to non-ergodicity of the displacement x); this in turn results in the remarkable difference of the temperature dependence of the ‘soft-mode’ frequency in the $B < 0$ and $B > 0$ cases. Sections 7 and 8 give the results of the numerical calculation of the dynamic response for the $\gamma = 0$ and $\gamma \neq 0$ cases respectively as functions of the temperature. The final section gives summary of the important conclusions obtained in the present work.

In carrying out the calculation below, the following units will often be used since they are most natural in the present problem.

$$\begin{aligned} \text{Energy} & \dots\dots\dots B^2/4A \\ \text{Temperature} & \dots\dots\dots B^2/4Ak_B \\ \text{Frequency} & \dots\dots\dots (2|B|/M)^{1/2} \\ \text{Susceptibility} & \dots\dots\dots 1/|B| \end{aligned}$$

§ 2. Formal expression for the classical dynamic susceptibility

In this section, we derive a formal expression for the classical dynamic susceptibility above Curie temperature using the linear-response theory. Further detailed calculation of the susceptibility will be continued in § 5.

Since we consider the system in the paraelectric phase exclusively, the canonical average $\langle x \rangle$ vanishes identically in Eq. (1.2) unless an external field is present. Suppose now that an alternating electric field E with angular frequency ω is applied upon the system. Then as far as the response linear in E is considered, $\langle x \rangle$ oscillates with the same angular frequency ω . We therefore regard H_1 defined by Eq. (1.2) as the external disturbance and apply the linear-response theory^{4,5)} to calculate $\langle x \rangle$. we then get

$$\langle x \rangle = \phi(\omega) [\gamma \langle x \rangle + E e^{-i\omega t}],$$

from which the dynamic susceptibility $\chi(\omega) = \langle x \rangle / E e^{-i\omega t}$ is expressed as

$$\chi(\omega) = \phi(\omega) / [1 - \gamma \phi(\omega)]. \tag{2.1}$$

$\phi(\omega)$ represents the classical dynamic polarizability of non-interacting oscillators.

When we decompose it into real and imaginary parts by $\phi(\omega) = \phi_1(\omega) + i\phi_2(\omega)$, they are given by

$$\phi_1(\omega) = \frac{1}{\pi} \text{v.p.} \int_{-\infty}^{+\infty} \frac{\phi_2(x)}{x - \omega} dx, \quad (2.2)$$

$$\phi_2(\omega) = \frac{\omega}{2k_B T} \int_{-\infty}^{+\infty} e^{i\omega t} \langle x(0)x(t) \rangle_0 dt, \quad (2.3)$$

where $\langle \dots \rangle_0$ means that we are to take the canonical average with respect to the Hamiltonian H_0 . It should be remembered here that our theory is classical. The above result can be obtained as the $\hbar\omega/k_B T \rightarrow 0$ limit of the corresponding quantum-mechanical expression.

Thus the further task to be made is to reduce Eq. (2.3) into an explicit form. It is done in §§ 4 and 5. Before proceeding to it, we discuss static properties of the system in the following section.

§ 3. Curie temperature and static susceptibility

Before going on to a rather detailed analysis of the dynamic susceptibility, we consider in this section the static susceptibility and Curie temperature.

The static susceptibility is obtained by putting $\omega=0$ in Eqs. (2.1) and (2.2):

$$\chi(0) = \phi(0) / [1 - \gamma\phi(0)], \quad (3.1)$$

$$\phi(0) = \langle x^2 \rangle_0 / k_B T. \quad (3.2)$$

The temperature T_C at which phase transition occurs is given by the solution of $1 - \gamma\phi(0) = 0$. An important quantity in the above equations is $\langle x^2 \rangle_0$. We show below how it can be calculated and show explicitly the temperature dependence of the static susceptibility and γ -dependence of the Curie temperature T_C .

To evaluate $\langle x^2 \rangle_0$, we introduce a new variable $y = (A/k_B T)^{1/4} x$ and a quantity

$$Z(p) = \int_{-\infty}^{\infty} \exp[-(y^4 + 2py^2)] dy \quad (3.3)$$

proportional to the partition function, where p is defined by

$$p = B(4Ak_B T)^{-1/2}. \quad (3.4)$$

The sign of p depends on whether the potential has one or two minima. In terms of $Z(p)$ defined in this way, the static polarizability is written

$$\phi(0) = -\frac{p}{B} \frac{d}{dp} \log Z(p), \quad (3.5)$$

irrespective of the sign of p (and hence of B).

Now the function $Z(p)$ can be expressed as

$$Z(p) = \frac{1}{2}\Gamma(\frac{1}{4})F(\frac{1}{4}, \frac{1}{2}; p^2) - \Gamma(\frac{3}{4})pF(\frac{3}{4}, \frac{3}{2}; p^2) \tag{3.6}$$

in terms of the gamma function Γ and the confluent hypergeometric function

$$F(\alpha, \gamma; z) = 1 + \frac{\alpha}{\gamma} \frac{z}{1!} + \frac{\alpha(\alpha+1)}{\gamma(\gamma+1)} \frac{z^2}{2!} + \dots \tag{3.7}$$

The above result can be perhaps most easily obtained by observing that $Z(p)$ satisfies the confluent hypergeometric differential equation

$$p^2 \frac{d^2Z}{d(p^2)^2} + \left(\frac{1}{2} - p^2\right) \frac{dZ}{dp^2} - \frac{1}{4}Z = 0,$$

or else by direct expansion of $Z(p)$ in powers of p .

For $|p| \ll 1$, the power series expression (3.7) is useful to calculate $Z(p)$. From Eqs. (3.5), (3.6) and (3.7), the static polarizability $\phi(0)$ in this limit is found to be

$$\phi(0) = \frac{2}{\sqrt{T}} \left[\delta - \frac{2}{\sqrt{T}} \left(\frac{1}{4} - \delta^2 \right) \cdot \text{sgn } B \right], \tag{3.8}$$

where $\delta \equiv \Gamma(3/4)/\Gamma(1/4) = 0.3380$ and the natural units given at the end of § 1 have been adopted. The symbol sgn means ‘the sign of’.

For $|p| \gg 1$ on the other hand, we use the asymptotic expansion formula⁶⁾ for the confluent hypergeometric function. The result becomes

$$\left. \begin{aligned} Z(p) &= (\pi/2p)^{1/2} G(\frac{1}{4}, \frac{3}{4}; -p^2) && \text{for } p > 0, \\ Z(p) &= (\pi/|p|)^{1/2} G(\frac{1}{4}, \frac{3}{4}; p^2) \exp(p^2) && \text{for } p < 0, \end{aligned} \right\} \tag{3.9}$$

where

$$G(\alpha, \gamma; z) = 1 + \frac{\alpha\gamma}{1!z} + \frac{\alpha(\alpha+1)\gamma(\gamma+1)}{2!z^2} + \dots$$

Thus in the limit $|p| \gg 1$, we get the following asymptotic formulae from Eqs. (3.5) and (3.9):

$$\phi(0) = \frac{1}{2} \left(1 - \frac{3}{4}T + \frac{3}{2}T^2 \right) \quad \text{for } B > 0, \tag{3.10}$$

$$\phi(0) = 2 \left(1 - \frac{1}{4}T \right) / T \quad \text{for } B < 0, \tag{3.11}$$

where again we have used our natural units.

Equations (3.8), (3.10) and (3.11) can be used to obtain the algebraic expressions for the Curie temperature and the static susceptibility $\chi(0)$ in the $T_c \ll 1$ and $T_c \gg 1$ limits; they are summarized in Table I.

Figure 2 shows^{*)} the Curie temperature plotted as a function of $\gamma/|B|$. The dashed line in the figure represents another quantity to be discussed later in § 6.

^{*)} In fact in carrying out these numerical calculations, Eqs. (3.6) and (3.9) were not sufficient to cover all the ranges of temperature. In the intermediate region, use was made of the other formulae which are to be derived in § 6.

Table I. Curie temperature and static susceptibility in the $T_C \gg 1$ and $T_C \ll 1$ cases. The units mentioned at the end of § 1 are used.

case	Curie temperature T_C	$\chi(0)$ for $T \sim T_C$
$T_C \gg 1$ ($\gamma \gg B $)	$0.457 \left(\frac{\gamma}{B}\right)^2 \left[1 - 2.38 \frac{B}{\gamma}\right]$	$\frac{0.914(\gamma/ B)}{T - T_C}$
$T_C \ll 1, B > 0$ ($\gamma \sim 2B$)	$\frac{8}{3} \left(\frac{1}{2} - \frac{B}{\gamma}\right)$	$\frac{4B/3\gamma}{T - T_C}$
$T_C \ll 1, B < 0$ ($\gamma \ll B $)	$\frac{2\gamma}{ B } \left(1 - \frac{\gamma}{2 B }\right)$	$\frac{2}{T - T_C}$

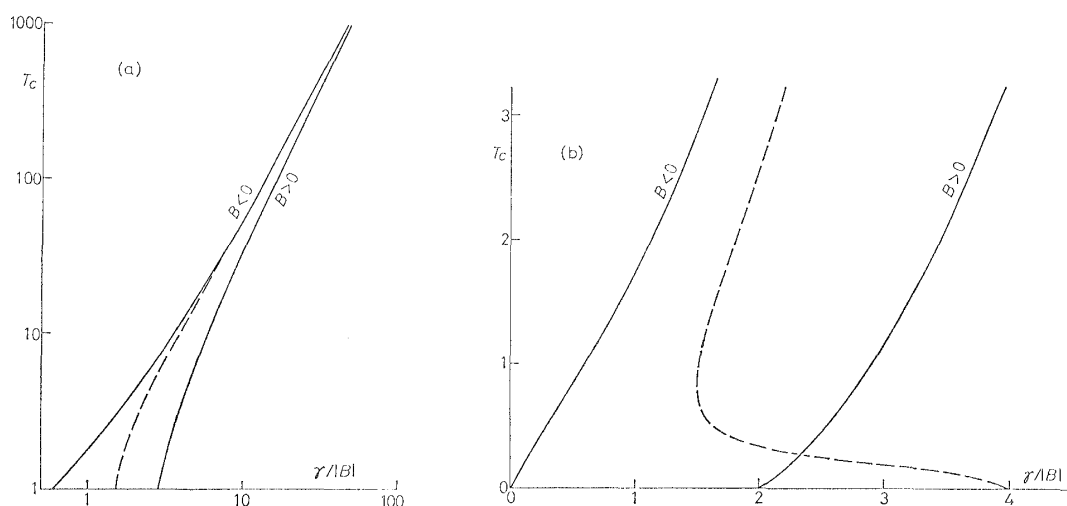


Fig. 2. Curie temperature (in units of $B^2/4Ak_B$) as a function of the ratio $\gamma/|B|$ for $B < 0$ (double-minimum potential) and $B > 0$ (single-minimum potential) cases. The dashed curve represents another characteristic temperature T_C' discussed in § 6.

As may be seen in the figure (or from Table I), the difference between the two curves decreases as $\gamma/|B|$ increases. This is indeed natural because at temperatures much higher than unity the term Bx^2 in the potential becomes unimportant.

On the other hand, around $T_C = 0$, they show different behaviour: in the $B < 0$ case, even a vanishingly small value of $\gamma/|B|$ is sufficient to cause the phase transition, whereas in the $B > 0$ case γ/B has to be greater than 2 in order to let the system undergo a phase transition. The difference stems from the quite different temperature dependence of $\langle x^2 \rangle_0$ in the two cases. In the former case, since the bottom of the potential is located not at the origin but at $x = (|B|/2A)^{1/2}$, $\langle x^2 \rangle_0$ tends to $|B|/2A$ at sufficiently low temperatures. As a result, one gets $T_C = 2\gamma/|B|$. In contrast to this, in the latter case, $\langle x^2 \rangle_0$ tends to $k_B T/2B$ as $T \rightarrow 0$, which requires γ/B to be greater than 2 in order that the phase transition take place. This is the reason for the different behaviour of the two curves about $T_C = 0$.

Our result for $B > 0$ appears to be in agreement with the previous one by Lines³⁾ which was obtained by direct numerical calculation of $\langle x^2 \rangle_0$, though the comparison is not easy since he plots $\sqrt{T_C B} / 2\gamma\delta$ versus $2B/\gamma$ (Fig. 1 of reference 3)).

Figure 3 shows^{*)} the inverse of static susceptibility for $T_C = 0$ as a function of temperature. The dashed curve does not concern us at the moment; it will be discussed in § 6. As may be seen from Eq. (3.1), the inverse of the susceptibility is defined by $\chi(0)^{-1} = \phi(0)^{-1} - \gamma$. Here the dependence of $\chi(0)^{-1}$ upon T and T_C are separately contained in $\phi(0)^{-1}$ and γ respectively. Therefore the curves of $\chi(0)^{-1}$ for arbitrary values of T_C can be readily obtained by vertical shifting of the curves in Fig. 3 so that they cut the abscissa at $T = T_C$.

It is important to note that the two curves for $B > 0$ and $B < 0$ have very similar temperature dependence. This means that we cannot easily distinguish between the $B > 0$ and $B < 0$ cases so far as we are observing only the static response.

Finishing here a brief excursion on the static susceptibility, we now get back to the calculation of the dynamic susceptibility.

§ 4. Solution for the free oscillation

In § 2, we have seen that the solution for the free oscillation is needed to evaluate the dynamic susceptibility. It is obtained in this section; the result is subsequently used in the succeeding section to calculate the dynamic susceptibility.

We wish to solve the classical equation of motion of an anharmonic oscillator

$$M\ddot{x} + 4Ax^3 + 2Bx = 0 \tag{4.1}$$

for the given initial values of x and \dot{x} at $t = 0$. Integration of Eq. (4.1) gives a constant of motion E ,

$$(M/2)\dot{x}^2 + Ax^4 + Bx^2 = E. \tag{4.2}$$

Hence the solution of Eq. (4.1) can be expressed formally as

$$t = \left(\frac{M}{2}\right)^{1/2} \int^x \frac{dx}{\sqrt{E - Ax^4 - Bx^2}}. \tag{4.3}$$

^{*)} See the footnote on page 1481.

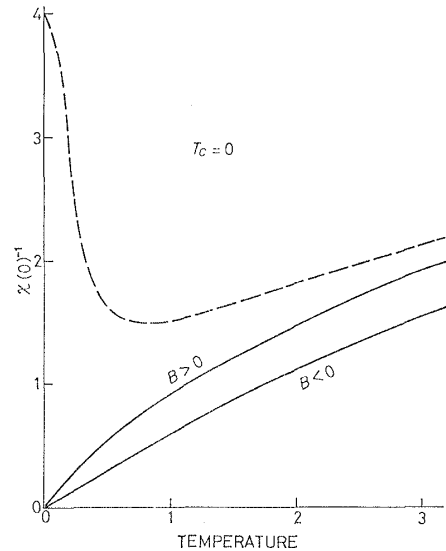


Fig. 3. Inverse of the static susceptibility in the $T_C \rightarrow 0$ limit plotted as a function of temperature. To get $\chi(0)^{-1}$ for a finite value of T_C , one has merely to shift the curve vertically so that it cross the abscissa at that value T_C . The dashed curve gives $\lim_{\omega \rightarrow 0} \chi(\omega)^{-1}$ for the $B < 0$ case discussed in § 6.

We now consider the $E > 0$ and $E < 0$ cases separately, since the oscillation is qualitatively different in these two cases.

Case I. $E > 0$ (B may be either positive or negative).

In this case, one can write

$$E - Ax^4 - Bx^2 = A(a^2 - x^2)(x^2 + b^2), \quad (4.4)$$

where a and b are real positive quantities defined by

$$a^2 = \frac{-B + \sqrt{B^2 + 4AE}}{2A}, \quad b^2 = \frac{B + \sqrt{B^2 + 4AE}}{2A}. \quad (4.5)$$

The motion of the oscillator is confined within the interval $(-a, a)$. In view of Eq. (4.4), we observe⁷⁾ that the integral (4.3) can be expressed in terms of the inverse function of the Jacobian elliptic function. The solution of the equation of motion (4.1) is thus given by

$$\begin{aligned} x(t) &= a \operatorname{cn}[\Omega t - \operatorname{cn}^{-1}(x/a)] \\ &= \frac{x \operatorname{cn} \Omega t + (\dot{x}/\Omega) \operatorname{sn} \Omega t \operatorname{dn} \Omega t}{1 - k^2(1 - x^2/a^2) \operatorname{sn}^2 \Omega t}, \end{aligned} \quad (4.6)$$

where x and \dot{x} denote their initial values at $t=0$, and Ω is given by

$$\Omega = \sqrt{\frac{2|B|}{M}} \left(1 + \frac{E}{4A}\right)^{1/4}. \quad (4.7)$$

sn , cn and dn represent the Jacobian elliptic functions, and their modulus k defined by

$$k^2 = \frac{a^2}{a^2 + b^2} = \frac{1}{2} \left(1 - \frac{\operatorname{sgn} B}{\sqrt{1 + E/(B^2/4A)}}\right) \quad (4.8)$$

measures the degree of anharmonicity of oscillation. In fact the sn , cn and dn functions depend on k , and hence should be written $\operatorname{sn}(\Omega t, k)$, etc.; but we omit the argument k to simplify the notation. In the $k \rightarrow 0$ limit (the limit of weak anharmonicity), the oscillation becomes harmonic, since $\operatorname{sn} \rightarrow \sin$, $\operatorname{cn} \rightarrow \cos$ and $\operatorname{dn} \rightarrow 1$.

The cn function is periodic in $4K(k)$, where $K(k)$ is the normal elliptic integral of the first kind,

$$K(k) = \int_0^{\pi/2} (1 - k^2 \sin^2 \theta)^{-1/2} d\theta.$$

The fundamental (angular) frequency of oscillation is therefore given by

$$\omega_f = 2\pi\Omega/4K(k). \quad (4.9)$$

Case II. $-B^2/4A < E < 0$ ($B < 0$).

In this case, the motion of the oscillator is confined within one of the potential wells and does not extend to the other. One can write

$$E - Ax^4 - Bx^2 = A(a^2 - x^2)(x^2 - c^2) \tag{4.10}$$

with use of

$$c^2 = -2E/|B| [1 + (1 + E/(B^2/4A))^{1/2}]$$

and a^2 already defined above. Substitution of Eq. (4.10) into Eq. (4.3) and an observation similar to the Case I yield

$$\begin{aligned} x(t) &= a \operatorname{dn}[\Omega' t - \operatorname{dn}^{-1}(x/a)] \\ &= \frac{x \operatorname{dn} \Omega' t + (\dot{x}/\Omega') \operatorname{sn} \Omega' t \operatorname{cn} \Omega' t}{1 - (1 - x^2/a^2) \operatorname{sn}^2 \Omega' t}, \end{aligned} \tag{4.11}$$

where, as in Case I, x and \dot{x} represent their initial values at $t=0$. Ω' is defined by

$$\Omega' = \sqrt{\frac{2|B|}{M} \left(\frac{1 + [1 + E/(B^2/4A)]^{1/2}}{2} \right)^{1/2}} \tag{4.12}$$

and the modulus of the elliptic functions by

$$k^2 = 1 - \frac{c^2}{a^2} = \frac{2}{1 + [1 + E/(B^2/4A)]^{-1/2}}. \tag{4.13}$$

Notice that the elliptic functions in Eqs. (4.6) and (4.11) have different modulus k .

Since the dn function is limited to $(1 - k^2)^{1/2} \leq \operatorname{dn} u \leq 1$, Eq. (4.11) represents the oscillation in the range $c \leq x \leq a$. Furthermore it is periodic in $2K(k)$. So, the fundamental (angular) frequency of oscillation is

$$\omega_f = 2\pi\Omega'/2K(k) \tag{4.14}$$

in this case.

As k^2 is an important quantity which measures the degree of anharmonicity, we show in Fig. 4 its dependence on the energy E , as calculated from Eqs. (4.8) and (4.13). In the $B > 0$ case, we have $0 \leq k^2 < 1/2$. Therefore the oscillation does not become highly distorted even for large values of the energy E . In contrast to this, the curve for $B < 0$ exhibits a peculiar behaviour. About $E=0$, the oscillation becomes quite distorted because it takes a long time for the oscillator to run in the neighbourhood of $x=0$. When the energy approaches $E=-1$, the oscillation becomes a harmonic

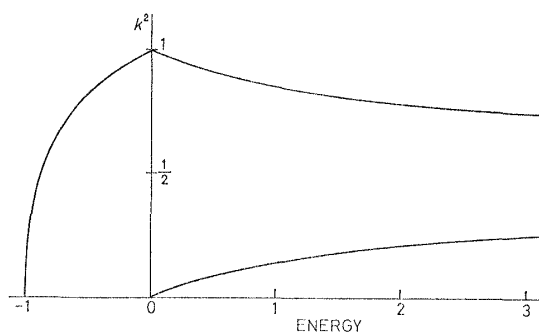


Fig. 4. Square of the modulus of the elliptic functions plotted as a function of the energy E (in units of $B^2/4A$). It is limited to $0 \leq k^2 \leq 1$ and measures the anharmonicity of oscillation,

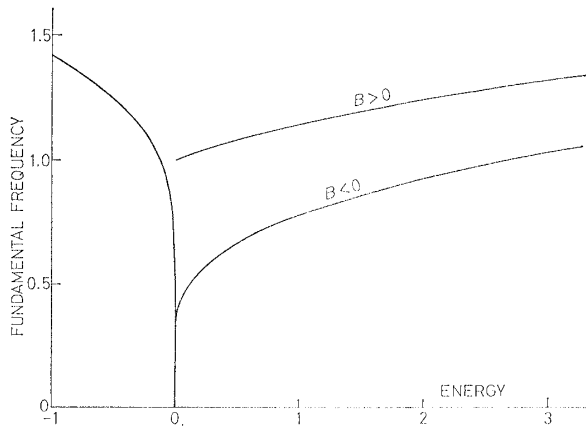


Fig. 5. Fundamental frequency (in units of $(2|B|/M)^{1/2}$) versus the energy E (in units of $B^2/4A$).

one about $x = (|B|/2A)^{1/2}$.

Figure 5 shows the dependence of the fundamental frequency upon the energy, computed by Eqs. (4.7), (4.8) and (4.9) for $E > 0$, and by Eqs. (4.12), (4.13) and (4.14) for $E < 0$. In the case $B > 0$, the fundamental frequency starts with the harmonic value 1.0 at $E = 0$ and gradually increases with E , with the energy dependence $1 + (3/16)E$ for $E \ll 1$. In the $E \gg 1$ limit, it approaches asymptotically

$$\left(\pi/2K\left(\frac{1}{\sqrt{2}}\right)\right)(1 + E)^{1/4} = 0.847(1 + E)^{1/4}.$$

In the $B < 0$ case too, the above asymptotic behaviour is valid. The peculiar energy-dependence about $E = 0$, $\pi/\log(64/E)$ for $E > 0$ and $2\pi/\log(-64/E)$ for $E < 0$, arises from the logarithmic singularity of the elliptic integral $K(k)$ at $k = 1$. In physical terms, it is because the oscillator has to spend lots of time in the region near $x = 0$ on account of the small kinetic energy available. For $E \sim -1$, the oscillation becomes a harmonic one with frequency $\sqrt{2}$. The value $\sqrt{2}$ results from the shape of the potential, which can be approximated by $2|B|(x - \sqrt{|B|/2A})^2 - B^2/4A$ about $x = (|B|/2A)^{1/2}$.

To conclude this section, we have shown that the solution for the free oscillation can be expressed as Eqs. (4.6) and (4.11) by means of the Jacobian elliptic functions. We have also examined some basic properties of this oscillation. These results will be used in the following sections to investigate the dynamic response of the system.

§ 5. Explicit expression for the dynamic polarizability

In this section, we combine the results obtained in § 2 and § 4 to get an explicit and exact formula for the imaginary part $\phi_2(\omega)$ of the dynamic polarizability.

The correlation function $\langle x(0)x(t) \rangle_0$ appearing in the expression (2.3) for $\phi_2(\omega)$ is written explicitly as

$$\langle x(0)x(t) \rangle_0 = \int_{-\infty}^{\infty} dx \int_{-\infty}^{\infty} d\dot{x} e^{-E/k_B T} x(t) x \bigg/ \int_{-\infty}^{\infty} dx \int_{-\infty}^{\infty} d\dot{x} e^{-E/k_B T} \quad (5.1)$$

in which $x(t)$ is to be replaced by the right-hand side of Eq. (4.6) or Eq. (4.11), according to the sign of the energy E . Upon this substitution, the contribution of the \dot{x} terms in Eqs. (4.6) and (4.11) vanishes because of the phase-space

integral in Eq. (5.1). Therefore we have merely to consider the x terms.

To perform the integration, we measure the temperature T in units of $B^2/4Ak_B$, and introduce a new set of variables (x, ϵ) in lieu of (x, \dot{x}) , where ϵ is defined by

$$\epsilon = E/(B^2/4A) = (M\dot{x}^2/2 + Ax^4 + Bx^2)/(B^2/4A).$$

Equation (5.1) becomes then

$$\langle x(0)x(t) \rangle_0 = \frac{\int_0^\infty d\epsilon e^{-\epsilon/T} \int_a dx x(t) x [\epsilon B^2/4A - Ax^4 - Bx^2]^{-1/2}}{\int_0^\infty d\epsilon e^{-\epsilon/T} \int_a dx [\epsilon B^2/4A - Ax^4 - Bx^2]^{-1/2}}. \tag{5.2}$$

The range of integration is $0 < \epsilon < \infty$, $0 < x < a$ for $B > 0$, and $-1 < \epsilon < \infty$, $c < x < a$ for $B < 0$. It is therefore convenient to treat the two cases separately.

5.1 The $B > 0$ case (single-minimum potential)

If one uses Eqs. (4.4), (4.6) and (4.8) in Eq. (5.2), and introduces $z = \text{cn}^{-1}(x/a)$, then one finds that

$$\langle x(0)x(t) \rangle_0 = \frac{\int_0^\infty d\epsilon e^{-\epsilon/T} a k \int_0^{K(k)} dz \text{cn}^2 z f_1(\Omega t, z)}{\int_0^\infty d\epsilon e^{-\epsilon/T} k K(k) / a}, \tag{5.3}$$

$$f_1(u, z) = \frac{\text{cn } u}{1 - k^2 \text{sn}^2 z \text{sn}^2 u}, \tag{5.4}$$

where a , Ω and k have already been defined by Eqs. (4.5), (4.7) and (4.8) respectively.

Before doing integration over z in Eq. (5.3), we first calculate its Fourier transform. For that purpose, Fourier transformation

$$\int_{-\infty}^\infty e^{i\omega t} f_1(\Omega t, z) dt = \frac{1}{\Omega} \int_{-\infty}^\infty e^{iu\omega/\Omega} f_1(u, z) du \tag{5.5}$$

has to be effected. The function $f_1(u, z)$ has simple poles at $u = \pm z + 2mK(k) + (2n+1)iK'(k)$, where m and n are integers, and $K'(k)$ is defined by

$$K'(k) = K(\sqrt{1-k^2}) = \int_1^{1/k} dx [(x^2-1)(1-k^2x^2)]^{-1/2}.$$

Table II. Poles and residues of the functions $f_1(u, z)$ and $f_2(u, z)$ defined by Eqs. (5.4) and (5.13) respectively.

pole	residue of f_1	residue of f_2
$z + 4mK + (2n+1)iK'$	$-\frac{i(-1)^n}{2k \text{cn } z}$	$-\frac{i(-1)^n}{2 \text{dn } z}$
$z + (4m+2)K + (2n+1)iK'$	+	-
$-z + 4mK + (2n+1)iK'$	-	-
$-z + (4m+2)K + (2n+1)iK'$	+	-

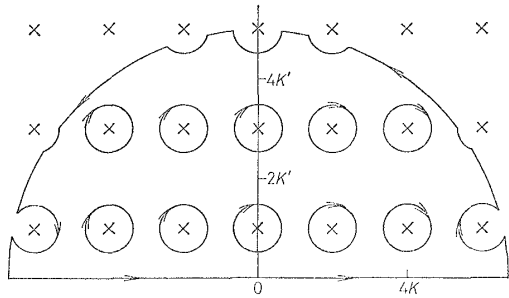


Fig. 6. Path on the complex u -plane to compute Fourier integral.

The periodic two-dimensional array of the simple poles on the complex u -plane is a direct consequence of the double periodicity of the Jacobian elliptic functions. The poles and residues of $f_1(u, z)$ are listed in Table II; they can be obtained by using some basic properties of the Jacobian elliptic functions. The integral (5.5) can then be evaluated by taking contour integral along the path shown in Fig. 6 on the upper half of the complex u -plane and letting the radius of the hemi-circle tend to infinity:

$$\int_{-\infty}^{\infty} e^{i\omega t} f_1(\Omega t, z) dt = \frac{2\pi}{kK \operatorname{cn} z} \sum_{n=-\infty}^{\infty} \frac{\cos[(2n+1)\pi z/2K]}{q^{n+1/2} + q^{-n-1/2}} \delta\left(\omega - \frac{(2n+1)\pi\Omega}{2K}\right),$$

in which

$$q = \exp(-\pi K'/K)$$

is referred to as the nome.

After the Fourier transformation has been effected in this way, we carry out the z -integration utilizing the formula

$$\int_0^K dz \operatorname{cn} z \cos\left[\left(n + \frac{1}{2}\right)\frac{\pi z}{K}\right] = \frac{\pi}{k} (q^{n+1/2} + q^{-n-1/2})^{-1}.$$

The final result becomes

$$\phi_2(\omega) = S_1(\omega) / Z_1, \tag{5.6}$$

$$Z_1 = \int_0^\infty d\varepsilon e^{-\varepsilon/T} K(k) / \Omega, \tag{5.7}$$

$$S_1(\omega) = \frac{4\pi^3}{T} \omega \int_0^\infty d\varepsilon e^{-\varepsilon/T} \frac{\Omega}{K(k)} \sum_{n=-\infty}^{\infty} (q^{n+1/2} + q^{-n-1/2})^{-2} \times \delta[\omega - (2n+1)\pi\Omega/2K(k)]. \tag{5.8}$$

Here use is made of the units mentioned at the end of § 1. We repeat the definition of Ω and k for the sake of completeness:

$$\begin{aligned} \Omega &= (1 + \varepsilon)^{1/4}, \\ k^2 &= \frac{1}{2}[1 - \operatorname{sgn} B \cdot (1 + \varepsilon)^{-1/2}]. \end{aligned} \tag{5.9}$$

The meaning of Eq. (5.8) is straightforward. The quantity $\Omega\pi/2K(k)$ means the fundamental frequency of the oscillation for a given energy ε , and the δ

function selects odd harmonics. The absence of even harmonics is related to the symmetry of the potential, $V(x) = V(-x)$. Since the fundamental frequency is no less than 1.0, the loss spectrum $\phi_2(\omega)$ gets a non-vanishing value for $\omega > 1$. Contribution of the third harmonic begins at $\omega = 3$.

The weighting factor

$$(q^{n+1/2} + q^{-n-1/2})^{-2} \tag{5.10}$$

gives the intensity of the harmonic specified by n . In the $T \rightarrow 0$ limit, the Boltzmann factor $e^{-\epsilon/T}$ makes only the $\epsilon \ll 1$ region significant. In that case, one has $q \rightarrow k^3/16 \cong \epsilon/64$, and the weighting factor (5.10) suppresses all the harmonics except the $n=0$ (and $n=-1$) one, yielding $\phi_2(\omega) = (\pi/4) [\delta(\omega-1) - \delta(\omega+1)]$.

In the other limit $T \gg 1$, the region $\epsilon \gg 1$ becomes important. One then has $k^2 \sim 1/2$ and $q \sim e^{-\pi}$. When one compares the intensity of the $n=1$ and $n=0$ harmonics for a fixed energy $\epsilon \gg 1$, then the ratio becomes $\sim e^{-2\pi} = 0.0019$. This means that the harmonics with $n \geq 1$ are not very essential in the dynamic response. The most important effect of the anharmonicity manifests itself in the dependence of the fundamental frequency upon the energy ϵ .

As shown in Eq. (2.2), the real part $\phi_1(\omega)$ of the polarizability is the Hilbert transform of the imaginary part $\phi_2(\omega)$ given by Eq. (5.6). We can examine its behaviour for $\omega \ll 1$ by expanding it in powers of ω . It is then found that $\phi_1(\omega)$ has the form

$$\phi_1(\omega) = \phi_1(0) + \alpha\omega^2. \tag{5.11}$$

α is a complicated quantity and is difficult to compute, even numerically, for general values of T . Only for $T \ll 1$, it can be calculated explicitly, and we have

$$\phi_1(\omega) = \frac{1}{2}(1 - \frac{3}{4}T + \frac{3}{8}T^2) + \frac{1}{2}\omega^2. \tag{5.12}$$

Here the first term on the right-hand side is the same as (3.10) obtained in § 3.

5.2 The $B < 0$ case (double-minimum potential)

In this case, the ϵ -integration in Eq. (5.2) can be divided into two parts: $-1 < \epsilon < 0$ and $0 < \epsilon < \infty$. Calculation of the latter part has no difference from the $B > 0$ case mentioned above except the difference of k^2 defined by Eq. (5.9).

The former part can be calculated parallel to the $B > 0$ case. One has merely to use Eqs. (4.10), (4.11) and (4.13) in Eq. (5.2) and define a new variable $z = \text{dn}^{-1}(x/a)$. The function which appears in an expression similar to (5.3) in place of f_1 is

$$f_2(u, z) = \frac{\text{dn } u}{1 - k^2 \text{sn}^2 z \text{sn}^2 u}. \tag{5.13}$$

This function has the same poles as f_1 , and they are listed in Table II together with the residues. Its Fourier transform can be computed by taking the contour integral along the same path. The calculation finishes up with the z -integration using the formula

$$\int_0^K dz \operatorname{dn} z \cos \frac{n\pi z}{K} = \frac{\pi}{q^n + q^{-n}},$$

and results in the following expression:

$$\phi_2(\omega) = [S_1(\omega) + S_2(\omega)]/[Z_1 + Z_2], \quad (5.14)$$

$$Z_2 = \int_{-1}^0 d\varepsilon e^{-\varepsilon/T} K(k)/\Omega', \quad (5.15)$$

$$S_2(\omega) = \frac{4\pi^3\omega}{T} \int_{-1}^0 d\varepsilon e^{-\varepsilon/T} \frac{\Omega'}{K(k)} \sum_{n=-\infty}^{\infty} (q^n + q^{-n})^{-2} \delta[\omega - n\pi\Omega'/K(k)], \quad (5.16)$$

where the units are those mentioned at the end of § 1. For the sake of completeness, we repeat the definition of Ω' and k in these units:

$$\Omega' = [(1 + \sqrt{1 + \varepsilon})/2]^{1/2}, \quad (5.17)$$

$$k^2 = 2\sqrt{1 + \varepsilon}/(1 + \sqrt{1 + \varepsilon}). \quad (5.18)$$

Z_1 and $S_1(\omega)$ have already been defined by Eqs. (5.7) and (5.8) respectively. Attention should be given here to the fact that they depend on the sign of B because of Eq. (5.9).

Equation (5.16) contains the $n=0$ term, but it drops out automatically on account of the common factor ω . The δ function now selects all the even and odd harmonics; this is because the potential has no symmetry about $x = (|B|/2A)^{1/2}$.

At sufficiently low temperatures only the $n=1$ (and $n=-1$) harmonic with frequency $\sim \sqrt{2}$ survives the weighting factor $(q^n + q^{-n})^{-2}$.

The real part $\phi_1(\omega)$ of the polarizability about $\omega=0$ has the form

$$\phi_1(\omega) = \lim_{\omega \rightarrow 0} \phi_1(\omega) + \beta\omega^2. \quad (5.19)$$

Here β is again a complicated quantity and can be calculated only for sufficiently low temperatures. For $T \ll 1$, it follows that

$$\phi_1(\omega) = \frac{1}{4}(1 + \frac{2}{3}T) + \frac{1}{8}\omega^2. \quad (5.20)$$

Attention should be paid to the difference between the first term on the right-hand side of Eq. (5.19) and the static susceptibility discussed in § 3 (Eq. (3.5)). For example, Eq. (5.20) does not agree with Eq. (3.11) in the $\omega \rightarrow 0$ limit. We continue to discuss this difference which occurs in the $B < 0$ case and its origin in the following section.

§ 6. Further considerations on the 'static' susceptibility

In the preceding section, we have shown how the imaginary part $\phi_2(\omega)$ of the dynamic polarizability can be calculated exactly. The purpose of this small section is to take the $\omega \rightarrow 0$ limit in that result and to compare it with the static polarizability that we have already discussed in § 3.

Let us first consider the $B > 0$ case. We use Eq. (5.6) in Eq. (2.2) and let $\omega \rightarrow 0$, then it follows that

$$\lim_{\omega \rightarrow 0} \phi_1(\omega) = \phi(0) = \frac{4}{Z_1 T} \int_0^\infty d\varepsilon e^{-\varepsilon/T} [E(k) - (1 - k^2) K(k)] \Omega, \quad (6.1)$$

where $E(k)$ is the normal elliptic integral of the second kind:

$$E(k) = \int_0^{K(k)} \text{dn}^2(u, k) du = \int_0^{\pi/2} (1 - k^2 \sin^2 \theta)^{1/2} d\theta.$$

In obtaining Eq. (6.1), the formula

$$\int_0^K \text{cn}^2 u du = \frac{\pi^2}{k^2 K} \sum_{n=-\infty}^{\infty} (q^{n+1/2} + q^{-n-1/2})^{-2} = k^{-2} [E - (1 - k^2) K]$$

turns out to be useful. The ‘static’ polarizability obtained in Eq. (6.1) agrees with the one derived independently in Eq. (3.5). In the actual numerical calculation of Figs. 2 and 3, Eq. (6.1) has been utilized to bridge the gap between the $T \gg 1$ and $T \ll 1$ limits.

In the case $B < 0$, a similar calculation leads to*)

$$\lim_{\omega \rightarrow 0} \phi_1(\omega) = \frac{4}{(Z_1 + Z_2) T} \left(\int_0^\infty d\varepsilon e^{-\varepsilon/T} [E(k) - (1 - k^2) K(k)] \Omega + \int_{-1}^0 d\varepsilon e^{-\varepsilon/T} [E(k) - \pi^2/4K(k)] \Omega' \right). \quad (6.2)$$

To obtain the second term in the bracket, the formula

$$\frac{\pi^2}{K} \sum_{n=-\infty}^{\infty} (q^n + q^{-n})^{-2} = E \quad (6.3)$$

has been used. The dashed curve in Fig. 3 shows the inverse of $\lim_{\omega \rightarrow 0} \phi_1(\omega)$ given by Eq. (6.2) as a function of temperature.

A problem now arises because it disagrees with the static value already obtained in § 3. The difference, which becomes pronounced at low temperatures, stems from whether or not one drops the $n = 0$ term in Eq. (6.3). Actually, the solid curve $B < 0$ in Fig. 3 has been computed by adding the $n = 0$ term to Eq. (6.2).

The occurrence of the $n = 0$ term is related to the fact that the correlation function $\langle x(0)x(t) \rangle_0$ has non-vanishing d.c. component, or that its long-time average $\lim_{t \rightarrow \infty} t^{-1} \int_0^t \langle x(0)x(t) \rangle_0 dt$ does not vanish, because the oscillating motion is restricted within one of the potential wells. It must be included in the isothermal polarizability $\phi(0)$, but it has nothing to do with the dynamic properties of the system (of non-interacting oscillators).

*) It should be remembered that the definition of k depends on the signs of B and ε , as seen from Eqs. (5.9) and (5.18). Similarly, Z_1 , defined by Eq. (5.7), depends on the sign of B because of Eq. (5.9).

In the sophisticated terms of statistical physics, it is said that the displacement x is 'non-ergodic' in such a case, and various other examples are known of such a difference.⁸⁾ The phenomenon should occur in general for multiple-minimum potential, since it is caused by the above-mentioned singularity of the correlation function.

$\phi(\omega)$ thus possesses a discontinuous leap at $\omega=0$. Which of the two ($\phi(0)$ or $\lim_{\omega \rightarrow 0} \phi(\omega)$) is observed in a particular low-frequency measurement depends on whether or not the system can be regarded to be in quasi-equilibrium under the applied field.

The dashed curve in Fig. 2 shows the virtual temperature at which $\lim_{\omega \rightarrow 0} \chi(\omega)$ diverges for $B < 0$, which will be denoted by T_C' , as a function of $\gamma/|B|$. Since this characteristic temperature is always smaller than T_C , the divergence does not actually take place. The difference between T_C and T_C' substantially diminishes with increase in T_C . We shall turn to this difference in § 8 in relation to the temperature dependence of the 'soft-mode' frequency.

In this section we have considered the discontinuity of $\phi(\omega)$ at $\omega=0$. If one takes account of the quantum-mechanical effect, the situation becomes somewhat different, since the oscillator can go over into the other potential well through the tunnelling effect. $\phi(\omega)$ then gets a resonance at the tunnelling frequency and joins continuously to $\phi(0)$. The difference is unimportant so far as the tunnelling frequency is much smaller than $(2|B|/M)^{1/2}$.

§ 7. Dynamic susceptibility of non-interacting oscillators

In this section we present the results of numerical calculation for $\phi(\omega)$ —the susceptibility of non-interacting anharmonic oscillators. They are used in the succeeding section to compute the imaginary part $\chi_2(\omega)$ of the susceptibility of interacting oscillators.

$\phi_2(\omega)$ is given by Eqs. (5·6) and (5·14) for $B > 0$ and $B < 0$ cases respectively. In the numerators of these expressions, there appear integrals of the following type:

$$\int d\varepsilon w(\varepsilon) \delta(\omega - g(\varepsilon)).$$

The actual numerical calculation has been carried out by transforming it to

$$w(\varepsilon_0) \left| \left(\frac{dg(\varepsilon)}{d\varepsilon} \right)_{\varepsilon=\varepsilon_0} \right|^{-1},$$

where ε_0 is the root of $\omega = g(\varepsilon_0)$, and can be obtained numerically by means of the Newton method.

The real part $\phi_1(\omega)$ can be computed by Hilbert transforming the imaginary part $\phi_2(\omega)$. The results are given in Fig. 7. The excellent agreement (to four places in most cases) between the static susceptibility thus obtained by numerical Hilbert transformation of $\phi_2(\omega)$ and the one obtained independently in § 3 demon-

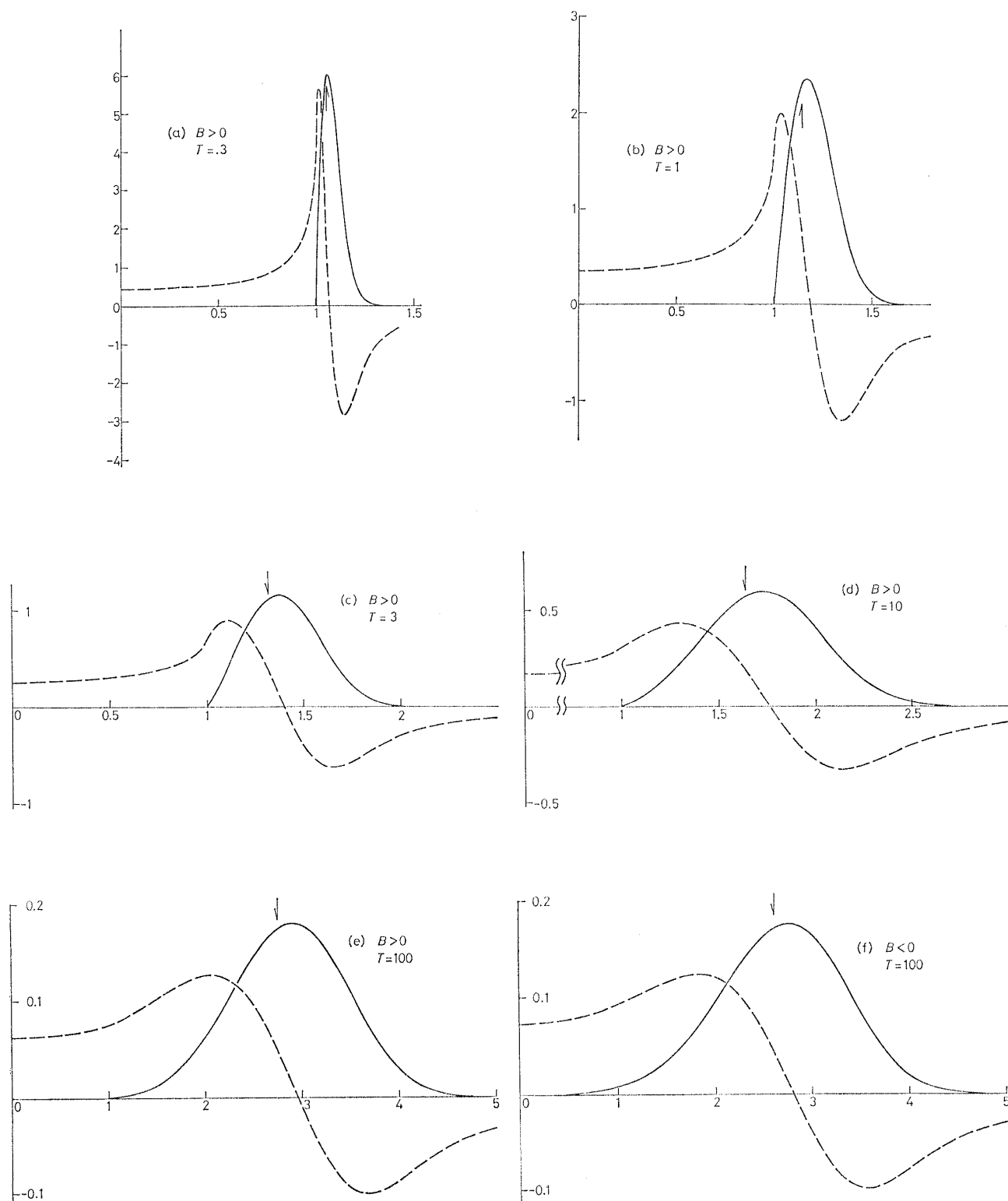


Fig. 7. Real part $\phi_1(\omega)$ (dashed line) and imaginary part $\phi_2(\omega)$ (solid line) of the dynamic susceptibility of non-interacting oscillators. The arrows indicate the value of the fundamental frequency of oscillation with energy $k_B T$.

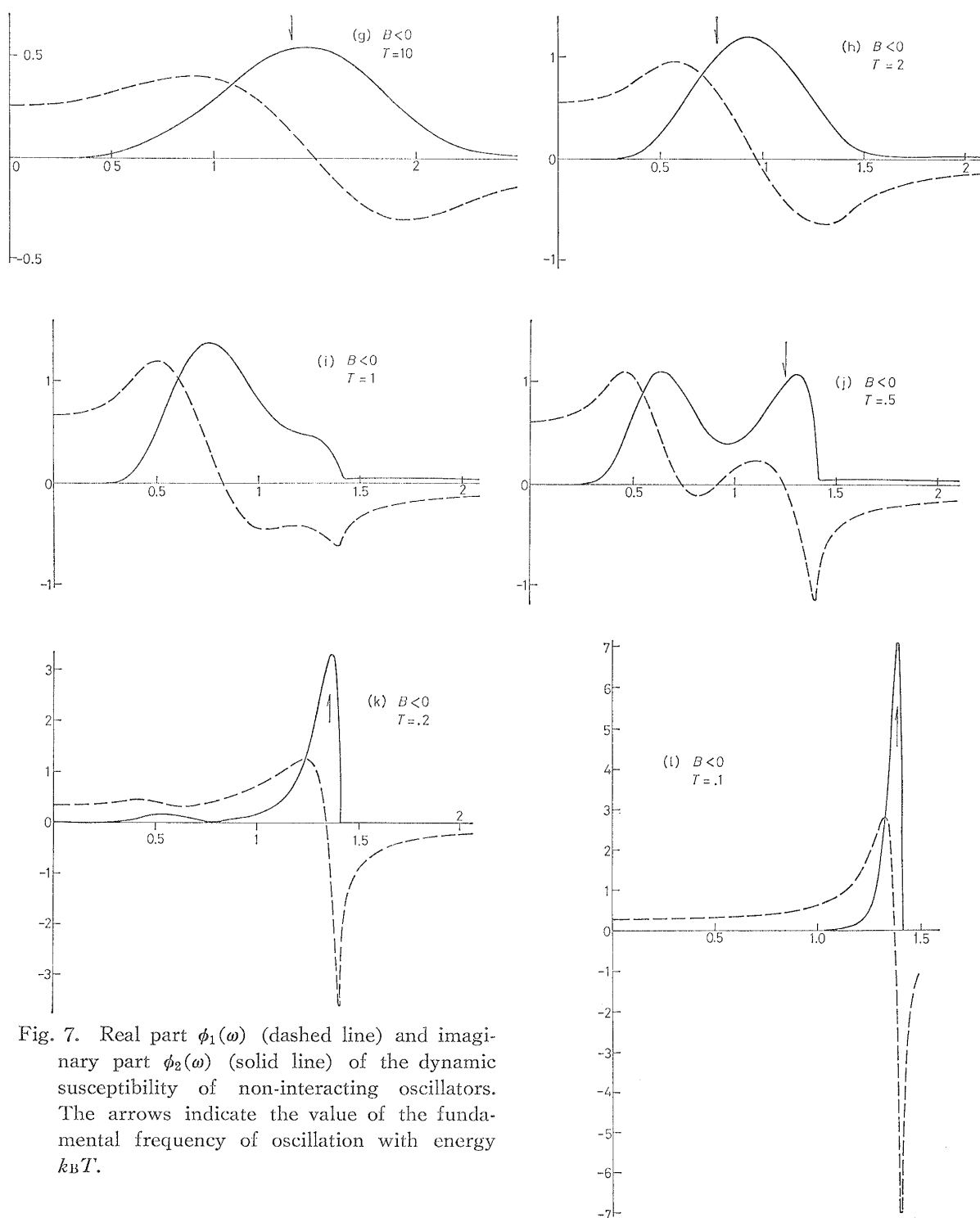


Fig. 7. Real part $\phi_1(\omega)$ (dashed line) and imaginary part $\phi_2(\omega)$ (solid line) of the dynamic susceptibility of non-interacting oscillators. The arrows indicate the value of the fundamental frequency of oscillation with energy $k_B T$.

states the high accuracy of the numerical work, to which considerable care has been taken.

The spectra for the single-minimum potential are given in Figs. 7(a) ~ 7(e). The imaginary part $\phi_2(\omega)$ vanishes identically for $\omega < 1.0$, since there can occur

no resonating oscillation for those frequencies. At low temperatures, the behaviour of $\phi(\omega)$ is similar to the response of harmonic oscillator. As temperature is raised, shift and broadening occur progressively. The broadening occurs for two reasons: one is the energy dependence of the frequency of oscillation. The other is the existence of various harmonics. The latter effect can occur only for $\omega > 3$ and is negligibly small compared with the contribution of the fundamental frequency. Therefore the shift and broadening of the response almost result from the energy dependence of the fundamental frequency of oscillation.

Figures 7(f) ~ 7(l) show the spectra for the double-minimum potential. The main part of the spectra is governed by the fundamental-frequency component, as in the single-minimum case. At sufficiently high temperatures, the spectra do not depend on the sign of B (compare Figs. 7(e) and 7(f)). It is because at such high temperatures only the term Ax^4 is dominant and that the term Bx^3 has little influence on the motion of the oscillator. As the temperature is lowered, the spectra exhibit the following characteristics which are absent in the $B > 0$ case:

(1) $\phi_2(\omega)$ does not vanish even for $\omega < 1$; As may be seen from Fig. 5, $\phi_2(\omega)$ cannot vanish for any frequency ω .

(2) A tail appears on the high-frequency side. The tail is due to the anharmonicity of the oscillation. As seen from Fig. 4, the anharmonicity becomes pronounced for $E \sim 0$, which means that the contribution of harmonics is greatest at intermediate temperatures $T \sim 1$, and that it is small at high and low temperatures.

(3) Double peak appears at intermediate temperature. Figure 5 tells us that for a given frequency ω , there correspond two oscillations—with positive and negative energies. At high temperatures the positive-energy response prevails, while at low temperatures the response tends to that of a harmonic oscillator with frequency $\sqrt{2}$. At intermediate temperatures, the two parts are competing; as a result, $\phi_2(\omega)$ has double peak and $\phi_1(\omega)$ shows a complex behaviour.

§ 8. Dynamic susceptibility of interacting oscillators

The imaginary part of the susceptibility can be written

$$\chi_2(\omega) = \frac{\phi_2(\omega)}{[1 - \gamma\phi_1(\omega)]^2 + \gamma^2[\phi_2(\omega)]^2}, \tag{8.1}$$

as may be seen from Eq. (2.1). We show below the behaviour of $\chi_2(\omega)$, using the $\phi_2(\omega)$ and $\phi_1(\omega)$ obtained in the preceding section and the relationship between γ and T_C obtained in § 3.

Let us begin with the $B > 0$ case. Figure 8 gives the temperature dependence of $\chi_2(\omega)$ spectra for $T_C = 2.5$ and $T_C = 40$. The resonance frequency lowers as the temperature approaches T_C . At temperatures near T_C , the peak manifests itself as a delta function in the $\omega < 1$ region. The frequency of such a collective

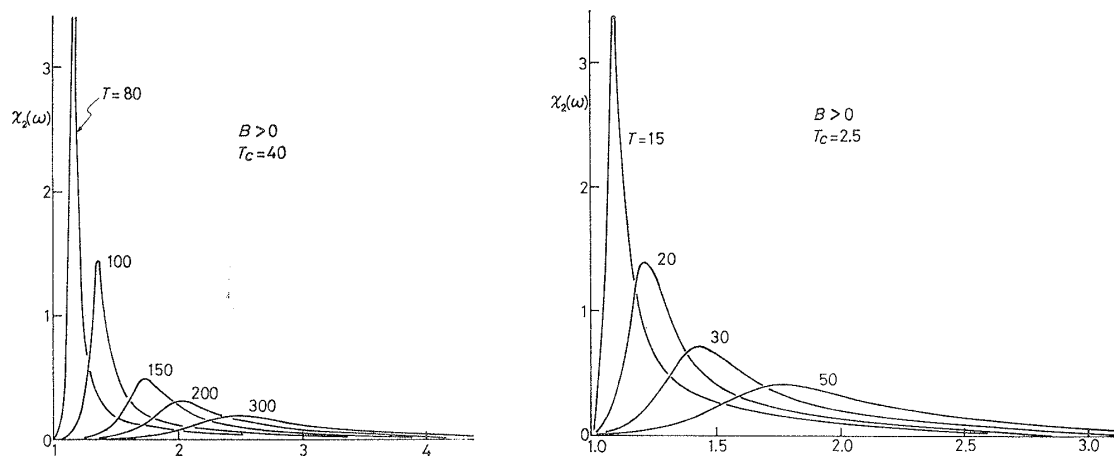


Fig. 8. Imaginary part $\chi_2(\omega)$ of dynamic susceptibility for the case of single-minimum potential.

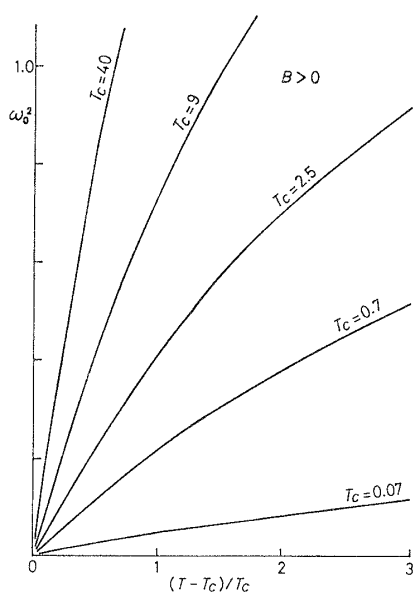


Fig. 9. Temperature dependence of the collective-mode frequency for the case of single-minimum potential.

mode is given by the solution of

$$\phi_1(\omega_0, T) = 1/\gamma = \phi_1(0, T_c). \quad (8.2)$$

The above equation explains the softening of the collective-mode frequency ω_0 as the temperature T approaches T_c . Using the expression (5.12) for $\phi_1(\omega, T)$ valid for $T \ll 1$ and $\omega \ll 1$, we get an expression for the soft-mode frequency

$$\omega_0 = \left[\frac{3}{4}(T - T_c)\right]^{1/2} \quad (8.3)$$

applicable to the $T_c \ll 1$ case. In Fig. 9 is shown the temperature dependence of ω_0^2 as obtained numerically. The curve for $T_c = 0.07$ satisfies Eq. (8.3) well.

Let us now go on to the $B < 0$ case. The collective-mode frequency is determined by Eq. (8.2) in this case too, but now a difference from the $B > 0$ case occurs because of the discontinuity of $\phi(\omega)$ at $\omega = 0$ mentioned in § 6.

The discontinuity does not guarantee that ω_0 tends to zero as $T \rightarrow T_c$; therefore softening of the collective mode does not take place in the $B < 0, T_c \lesssim 1$ case, in agreement with the conclusion of Vaks et al.¹⁾ Figure 10 shows the temperature dependence of the $\chi_2(\omega)$ spectra. For large T_c , the behaviour of $\chi_2(\omega)$ becomes qualitatively similar to the $B > 0$ case and the collective-mode frequency becomes highly temperature-dependent.

In Fig. 11 is plotted the peak frequency of the $\chi_2(\omega)$ spectra computed numerically. For large T_c , we have

$$\omega_0^2 \propto T - T_c',$$

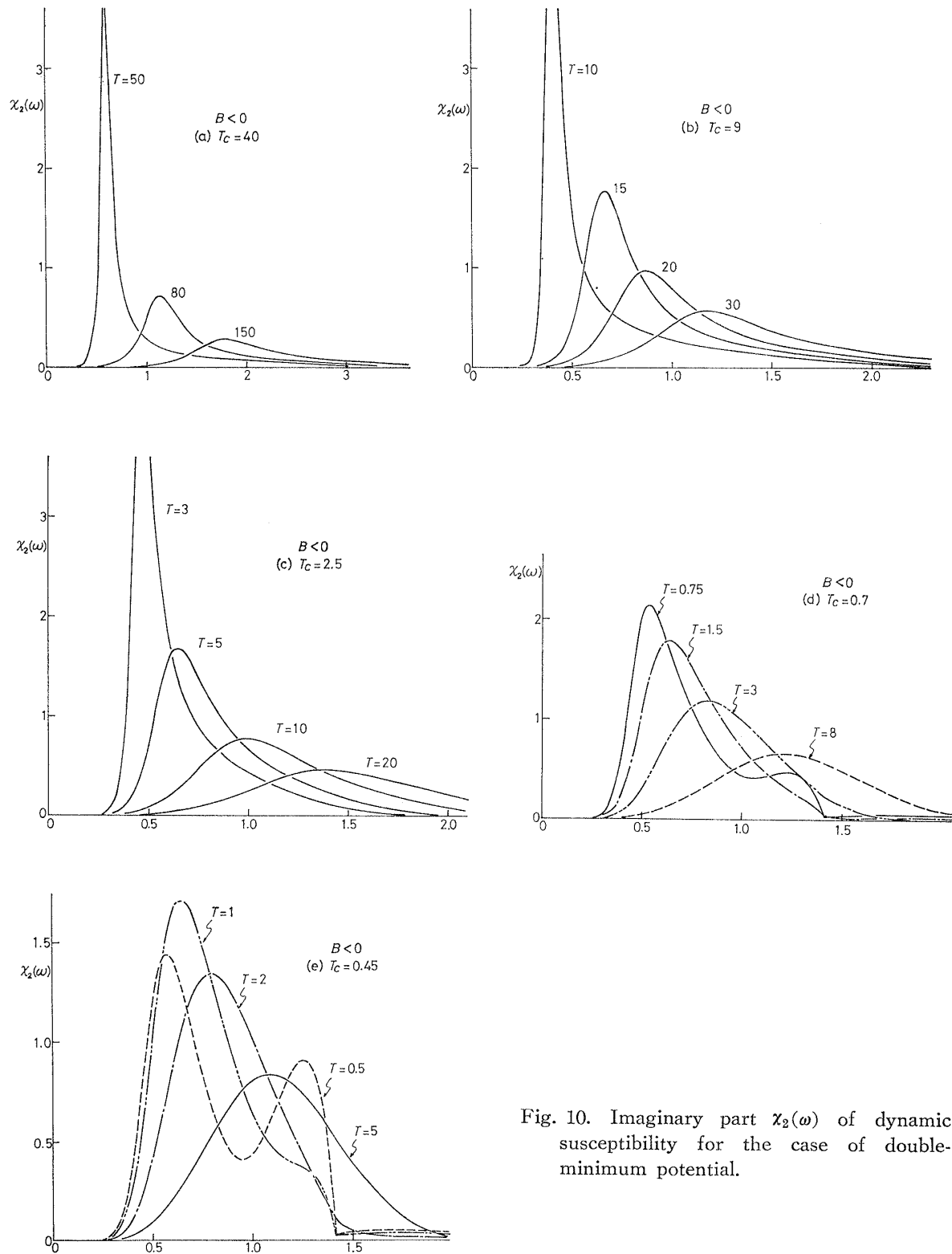


Fig. 10. Imaginary part $\chi_2(\omega)$ of dynamic susceptibility for the case of double-minimum potential.

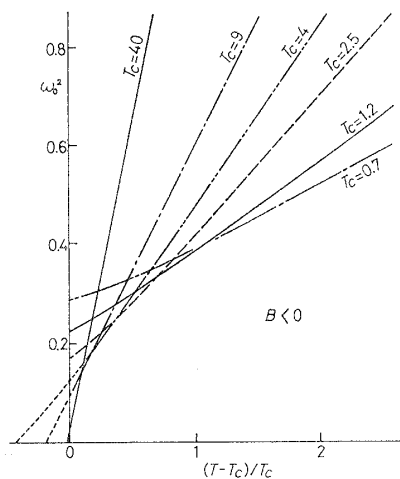


Fig. 11. Temperature dependence of the peak frequency of $\chi_2(\omega)$ for the case of double-minimum potential.

where T_c' is defined as the temperature at which $\lim_{\omega \rightarrow 0} \chi(\omega)$ virtually diverges and is shown graphically in Fig. 2. The curves in Fig. 11 cut the abscissa at $T = T_c' < T_c$ rather than at $T = T_c$. It looks as if the system were undergoing first-order phase transition, although the transition is actually of second order. For high T_c , the difference between T_c' and T_c (and hence the discontinuity of $\phi(\omega)$ at $\omega = 0$) diminishes; the collective mode then softens. For low T_c , the discontinuity becomes substantial, as a result there exist no anomalous oscillations. Our model thus correctly describes and connects these two limits of high and low Curie temperature.

§ 9. Conclusion

In this paper, we have considered a simple anharmonic oscillator system and have shown that its dynamic susceptibility above the Curie temperature can be calculated exactly. Although the theory has two restrictions—use of the Weiss molecular-field approximation and neglect of the quantum-mechanical effects, no approximations have been made otherwise. In particular, the anharmonicity of the potential is perfectly taken into account.

Important conclusions obtained in the present work may be summarized as follows:

(1) In the dynamic response, contribution of the fundamental-frequency component prevails over that of higher-harmonic components in both $B > 0$ and $B < 0$ cases. This means that the effect of the anharmonicity is reflected mainly on the energy dependence of the fundamental frequency of oscillation. Contribution of the higher harmonics can safely be neglected.

(2) In the $B > 0$ (single-minimum potential) case, which corresponds to the displacive ferroelectrics, the collective oscillation has a frequency proportional to $(T - T_c)^{1/2}$ near T_c .

(3) In the $B < 0$ (double-minimum potential) case, the dynamic response depends heavily upon the magnitude of T_c . If $k_B T_c$ is much greater than the height of the potential barrier $B^2/4A$, then the system may be regarded as displacive type. The frequency of collective oscillation is proportional to $(T - T_c')^{1/2}$, where T_c' is somewhat smaller than T_c . It looks as though the system underwent a first-order phase transition despite the fact that the transition is really of second order. The difference between T_c' and T_c results from the disconti-

nity of $\phi(\omega)$ at $\omega=0$, which in turn arises from the non-vanishing d.c. component of the correlation function $\langle x(0)x(t) \rangle_0$.

The discontinuity becomes substantial when $k_B T_C \ll B^2/4A$, to which case order-disorder ferroelectrics correspond. There exist no 'soft' modes in this case. We have not considered the tunnelling effects since the present theory is classical; but allowance for them does not change the conclusion, so far as the tunnelling frequency is much smaller than $(2|B|/M)^{1/2}$.

We have thus been able to describe the dynamic response of the high T_C (displacive type) and low T_C (order-disorder type) cases and the intermediate cases in terms of a unified anharmonic oscillator model.

Acknowledgments

The author expresses his sincere gratitude to Professor T. Matsubara, Dr. K. Yoshimitsu and Professor Y. Yamada for valuable enlightening discussions. The support of the Sakkokai Foundation is gratefully acknowledged. Thanks are also due to the staff of the Data Processing Center, Kyoto University, for use of its computing facilities.

References

- 1) V. G. Vaks, V. M. Galitskii and A. I. Larkin, *Zh. Eksp. i Teor. Fiz.* **51** (1966), 1592.
- 2) K. Aizu, *J. Phys. Soc. Japan* **21** (1966), 1240.
- 3) M. E. Lines, *Phys. Rev.* **177** (1969), 797.
- 4) R. Kubo, *J. Phys. Soc. Japan* **12** (1957), 570.
- 5) D. N. Zubarev, *Uspekhi Fiz. Nauk SSSR* **71** (1960), 71.
- 6) See, for example, L. D. Landau and E. M. Lifshits, *Kvantovaya Mekhanika* (Fizmatgiz, Moskow, 1963), Appendix d, Confluent hypergeometric function.
- 7) A number of useful formulae concerning the elliptic functions are compiled by P. F. Byrd and M. D. Friedman, *Handbook of Elliptic Integrals for Engineers and Scientists* (Springer-Verlag, 1954).
- 8) M. Suzuki, to be published in *Physica*.